Geoscientific
Model Development

Developing and optimizing shrub parameters representing sagebrush (*Artemisia* spp.) ecosystems in the northern Great Basin using the Ecosystem Demography (EDv2.2) model

Karun Pandit[1], Hamid Dashti[1], Nancy F. Glenn[1], Alejandro N. Flores[1], Kaitlin C. Maguire[2], Douglas J. Shinneman[2], Gerald N. Flerchinger[3], and Aaron W. Fellows[3]

[1]Department of Geosciences, Boise State University, 1910 University Dr, Boise, ID 83725-1535, USA
[2]United States Geological Survey, Forest and Rangeland Ecosystem Science Center, 970 Lusk St., Boise, ID 83706, USA
[3]United States Department of Agriculture, Agricultural Research Service, 800 Park Blvd., Suite 105, Boise, ID 83712, USA

Correspondence: Karun Pandit (karunpandit@gmail.com)

Abstract. Ecosystem dynamic models are useful for understanding ecosystem characteristics over time and space because of their efficiency over direct field measurements and applicability to broad spatial extents. Their application, however, is challenging due to internal model uncertainties and complexities arising from distinct qualities of the ecosystems being analyzed. The sagebrush-steppe ecosystem in western North America, for example, has substantial spatial and temporal heterogeneity as well as variability due to anthropogenic disturbance, invasive species, climate change, and altered fire regimes, which collectively make modeling dynamic ecosystem processes difficult. Ecosystem Demography (EDv2.2) is a robust ecosystem dynamic model, initially developed for tropical forests, that simulates energy, water, and carbon fluxes at fine scales. Although EDv2.2 has since been tested on different ecosystems via development of different plant functional types (PFT), it still lacks a shrub PFT. In this study, we developed and parameterized a shrub PFT representative of sagebrush (*Artemisia* spp.) ecosystems in order to initialize and test it within EDv2.2, and to promote future broad-scale analysis of restoration activities, climate change, and fire regimes in the sagebrush-steppe ecosystem. Specifically, we parameterized the sagebrush PFT within EDv2.2 to estimate gross primary production (GPP) using data from two sagebrush study sites in the northern Great Basin. To accomplish this, we employed a three-tier approach. (1) To initially parameterize the sagebrush PFT, we fitted allometric relationships for sagebrush using field-collected data, information from existing sagebrush literature, and parameters from other land models. (2) To determine influential parameters in GPP prediction, we used a sensitivity analysis to identify the five most sensitive parameters. (3) To improve model performance and validate results, we optimized these five parameters using an exhaustive search method to estimate GPP, and compared results with observations from two eddy covariance (EC) sites in the study area. Our modeled results were encouraging, with reasonable fidelity to observed values, although some negative biases (i.e., seasonal underestimates of GPP) were apparent. Our finding on preliminary parameterization of the sagebrush shrub PFT is an important step towards subsequent studies on shrubland ecosystems using EDv2.2 or any other process-based ecosystem model.

1 Introduction

Ecosystem dynamic models have been widely used to estimate terrestrial carbon flux and to project ecosystem characteristics over time and space (Dietze et al., 2014; Fisher et al., 2018), largely due to their efficiency over direct field measurements and their applicability to broad spatial scales. However, these models have also been associated with high levels of internal uncertainty and questions regarding their applicability to distinct and often complex ecosystems at large scale (Kwon et al., 2008). Sagebrush (*Artemisia* spp.) ecosystems in western North America provide a good exam-

ple of these types of modeling challenges, as these ecosystems are spatially heterogeneous and shaped by complex dynamics over time. Sagebrush ecosystems hold both high ecological and socioeconomic value, but they have been reduced to nearly half of their historical range and are declining at an alarming rate (Knick et al., 2003; Schroeder et al., 2004). Various factors have contributed to this decline, including land clearing, invasion of nonnative species such as cheatgrass (*Bromus tectorum*), and climate change, that have collectively altered vegetation composition, hydrological function, and wildfire frequency (Bradley, 2010; Connelly et al., 2004; McArthur and Plummer, 1978; Schlaepfer et al., 2014). In an attempt to restore portions of the sagebrush ecosystem, land managers have focused on reducing flammable vegetation, controlling invasive species, and seeding native plant species (Chambers et al., 2014; McIver and Brunson, 2014). There are relatively few studies that have evaluated carbon flux in sagebrush ecosystems in response to prescribed fire or restoration activities, and most of them used observational data from eddy covariance (EC) stations. However, given the large spatial extent of the sagebrush biome ($> 500\,000\,km^2$; Miller et al., 2011) and the paucity of EC station sites in sagebrush landscapes, the function of this ecosystem remains poorly understood, especially as management activities, fire, climate change, and invasive species continue to alter ecosystem structure, composition, and spatiotemporal dynamics.

Ecosystem Demography (EDv2.2) is a process-based ecosystem dynamic model that approximates the behavior of ensembles of size and age-structured individual plants to capture subgrid level ecosystem heterogeneity using partial differential equations (Medvigy et al., 2009; Moorcroft et al., 2001). This model was originally developed to study tropical ecosystems with trees as a primary component, but it has since been modified and applied to several different ecosystems, including boreal forests (Trugman et al., 2016) and temperate forests (Antonarakis et al., 2014; Medvigy et al., 2009, 2013). However, its application to semiarid shrubland ecosystems has not been explored and it lacks a shrub plant functional type (PFT) to study these ecosystems. Thus, we developed and parameterized a sagebrush PFT for EDv2.2, and used it to estimate gross primary production (GPP) for the sagebrush ecosystems in the Reynolds Creek Experimental Watershed (RCEW) located in the northern Great Basin of the United States, a cold-desert region dominated by expansive, shrub-steppe ecosystems.

In this study, our primary objective was to develop preliminary sagebrush PFT parameters in EDv2.2 and to constrain uncertainties through optimization of selected PFT parameters. To accomplish this, we employed a three-tiered approach. First, we parameterized the sagebrush PFT, by fitting allometric relationships for sagebrush using field-collected data, information from existing sagebrush literature, and borrowing parameters from other land models. Second, to identify the most influential parameters in GPP prediction, we

used a sensitivity analysis and identified the five most sensitive parameters affecting changes in GPP estimates. Third, to improve upon and assess model performance, we optimized the five most sensitive parameters using an exhaustive search method to estimate GPP and then compared the results with observations from two eddy covariance (EC) sites in the study areas. Our preliminary parameterization of the sagebrush shrub PFT is an important first step towards further study of shrubland ecosystem function using EDv2.2 or similar process-based ecosystem models.

2 Material and methods

2.1 Ecosystem Demography (EDv2.2) model

EDv2.2 is a process-based terrestrial biosphere model that occupies a mid-point on the continuum of individual-based (or gap) to area-based (or big-leaf) models (Fisher, 2010; Smith et al., 2001). Area-based models like LPJ-DGVM (Lund-Potsdam-Jena Dynamic Vegetation Model) (Sitch et al., 2003) and BIOME BGC (Running and Hunt, 1993, as cited in Bond-Lamberty et al., 2015) represent plant communities with area-averaged representation of a PFT for each grid cell. The simplification and computational efficiency of these models make them widely applicable for regional ecosystem analysis; however, this advantage often comes with a limited ability to properly capture light competition and competitive exclusion (Fisher, 2010; Bond-Lamberty et al., 2015; Smith et al., 2001). In contrast, individual-based models (IBMs), such as JABOWA (Botkin et al., 1972) and SORTIE (Pacala et al., 1993), represent vegetation at the individual plant level, thus making it possible to incorporate community processes like growth, mortality, recruitment, and disturbances. Recent improvements in computational efficiency have permitted the use of IBMs beyond traditional applications confined to limited spatial and temporal scales. EDv2.2 is a cohort-based model where individual plants with similar properties, in terms of size, age, and function, are grouped together to reduce the computational cost while retaining most of the dynamics of IBMs. Each cohort is defined by a PFT, number of plants per unit area, and dimensions of a single representative plant like diameter, height, structural biomass, and live biomass (Fisher et al., 2010). The cohort-based modeling approach in EDv2.2 has been applied to capture detailed ecological processes in studies investigating the effects of fire, drought, insect infestations, and climate effects on ecosystems at broad spatial scales (Fisher et al., 2018).

The land surface in EDv2.2 is composed of a series of gridded cells, which experience meteorological forcing from corresponding gridded data or from a coupled atmospheric model (Medvigy, 2006). The mechanistic scaling from individual to the region is achieved through size and age structured partial differential equations that closely approximate mean behavior of a stochastic gap model (Medvigy et al.,

Table 1. Parameters used to explore model performance for sagebrush PFT.

Parameter	Description	Unit
Maximum carboxylation rate (V_{m0})	Maximum carboxylation rate at 15 °C	$\mu\text{mol m}^{-2}\,\text{s}^{-1}$
Stomatal slope (M)	Slope of stomatal conductance–photosynthesis relationship	–
Cuticular conductance (b)	Intercept of stomatal conductance–photosynthesis relationship	$\mu\text{mol m}^{-2}\,\text{s}^{-1}$
Water conductance (K_w)	Supply coefficient for plant water uptake	ms^{-1} kg C per root
Leaf width (W_{leaf})	Controls leaf boundary layer conductance (m)	m
SLA	Specific leaf area	$\text{m}^2\,\text{kg}^{-1}$
GRF (r_g)	Growth respiration factor	–
Q ratio (q)	Ratio of fine roots to leaves	–
Leaf turnover rate (α_{leaf})	Inverse of leaf life span	Per annum (a^{-1})
Fine root turnover rate (α_{root})	Inverse of fine root life span	Per annum (a^{-1})
Storage turnover rate ($\alpha_{storage}$)	Turnover rate of plant storage pools	Per annum (a^{-1})

2009; Moorcroft et al., 2001). Each grid cell is subdivided into a series of dynamic horizontal tiles, which represent locations that experience similar disturbance history and have an explicit vertical canopy structure. This mechanism helps capture both vertical and horizontal distributions of vegetation structure and compositional heterogeneity compared to area-based models (Kim et al., 2012; Moorcroft et al., 2001, 2003; Sellers et al., 1992). EDv2.2 consists of multiple submodels for plant growth and mortality, phenology, disturbance, biodiversity, hydrology, land surface biophysics, and soil biogeochemistry to predict short-term and long-term ecosystem fluxes and to represent natural and anthropogenic disturbances (Kim et al., 2012; Medvigy et al., 2009; Zhang et al., 2015). Submodels in EDv2.2 rely mostly on many PFT-specific parameters, representing unique attributes of that particular group of species, to define the stated biological processes (Knox et al., 2015). Studies on shrub parameterization have been performed in LPJ-GUESS for the tundra region (Miller and Smith, 2012; Wolf, 2008); however, parameterization for shrub PFT is lacking for semiarid shrubland ecosystems. EDv2.2 has parameters defined for 17 different PFTs including grasses (C_3 and C_4), conifers, deciduous trees (temperate and tropical), and agricultural crops. In this study, we identified parameters for the sagebrush (shrub) ecosystem to simulate it in the model as a new PFT. We limited the scope of this study to sagebrush PFT parameterization using model structures and processes adopted in EDv2.2 for trees (e.g., seed dispersal, competition, mortality, and phenology), which we assumed would be generally applicable to shrubs (Wolf et al., 2008). Because we explored model performance based on GPP estimates, we selected 11 different parameters related to plant ecophysiology and biomass allocation to conduct sensitivity and optimization assessments (Table 1). We mainly relied on similar studies (Dietze et al., 2014; Fisher et al., 2010; LeBauer et al., 2013; Medvigy et al., 2009; Mo et al., 2008; Pereira et al., 2017), our preliminary sensitivity analyses, and consultation with other developers and users of the EDv2.2 model to select the parameters.

Detailed descriptions of submodels of EDv2.2 are available in existing literature (Medvigy et al., 2009; Moorcroft et al., 2001); thus, here we describe the ones related to the parameters used in this study. The ecophysiological submodel has a coupled photosynthesis and stomatal conductance scheme developed by Farquhar and Sharkey (1982) and Leuning (1995), respectively, and which estimates leaf-level carbon and water fluxes. Leaf-level carbon demand of C_3 plants is determined by the minimum of light-limited rate (J_e) and Rubisco-limited rate (J_c), and V_{m0} controls the latter as given by Eq. (1) after being scaled to a given temperature.

$$J_c = \frac{V_m(T_v)(C_{inter} - \tau)}{C_{inter} + K_1(1 + K_2)}, \tag{1}$$

where $V_m(T_v)$ is the maximum capacity of Rubisco to perform its carboxylase function at a given temperature T_v, scaled from V_{m0} using an exponential function (Medvigy et al., 2009) given below (Eq. 2); C_{inter} is the intercellular CO_2 concentration; τ is the compensation point for gross photosynthesis; K_1 is the Michaelis–Menten coefficient for CO_2; and K_2 is proportional to the Michaelis–Menten coefficient for O_2.

$$V_m(T_v) =$$

$$V_{m0}\frac{\exp\left(3000\left(\frac{1}{288.15} - \frac{1}{T_v}\right)\right)}{(1 - \exp\left(0.4\left(T_{v,lo} - T_v\right)\right))(1 + \exp(0.4\left(T_v - 318.15\right)))}, \tag{2}$$

where T_v is any given temperature for which the scaling is being done and $T_{v,lo}$ is the lower cutoff temperature.

Stomatal conductance, which is modeled using Leuning (1995), a variant of the Ball–Berry model (Eq. 3), is influenced by *stomatal slope* and *cuticular conductance*.

$$g_{sw} = \frac{MA_o}{(C_s - \tau)\left(1 + \frac{D_s}{D_0}\right)} + b, \tag{3}$$

Table 2. Coefficients for sagebrush (shrub) PFT to allometric equations in EDv2.2 (temperate PFTs).

Relationship	Equation	Coefficients
DBH (cm) to height (m)	$Ht = a(1 - e^{b \times DBH})$	$a = 4.7562, b = -0.002594$
DBH (cm) to woody biomass (kg)	$WB = \frac{a}{C2B} \times DBH^b$	$a = 5.709 \times 10^{-8}, b = 4.149$
DBH (cm) to leaf biomass (kg)	$LB = \frac{a}{C2B} \times DBH^b$	$a = 2.582 \times 10^{-6}, b = 2.746$
DBH (cm) to canopy area (m^2)	$CA = a \times DBH^b$	$a = 6.35 \times 10^{-5}, b = 2.18$
DBH (cm) to volume (m^3)	$V = a \times Ht \times DBH^b$	$a = 2.035 \times 10^{-5}, b = 2.314$
Volume (m^3) to root depth (m)	$D = a \times V^b$	$a = -3.0, b = 0.15$
DBH (cm) to wood area index	$WAI = n_{plant} \times a \times DBH^b$	$a = 0.0096, b = 2.0947$

DBH is diameter at breast height; Ht is height; WB is woody biomass; C2B is carbon to biomass ratio; LB is leaf biomass; CA is canopy area; V is volume; D is root depth; and WAI is wood area index.

where g_{sw} is stomatal conductance for water, A_o is photosynthetic rate, M is *stomatal slope*, b is *cuticular conductance*, D_0 is empirical constant, D_s is water vapor deficit, C_s is CO_2 concentration within leaf boundary, and τ is as described above. Stomatal control is also affected by the soil moisture supply term, which is a function of soil moisture, fine root biomass, and *water conductance*. When the available water supply is less than the demand predicted by the photosynthesis–conductance model, then photosynthesis, transpiration, and stomatal conductance are all linearly weighted down to match the supply (Dietze et al., 2014).

Water and CO_2 concentrations within the leaf boundary layer are influenced by *leaf width* along with other factors like wind speed, leaf area index, and molecular diffusivity of heat. *Specific leaf area* (SLA) has units of leaf area per unit leaf carbon and is used to scale up leaf-level to canopy-level fluxes. Relationships between growth respiration and net photosynthesis are controlled by the *growth respiration factor*. In EDv2.2, while leaf biomass is determined by the PFT-specific allometric equation (as shown in Table 2 for sagebrush) based on diameter, fine root biomass is defined by a *ratio of leaves to fine roots*. *Leaf turnover* and *fine root turnover* rates together influence overall litter turnover rate, even though in deciduous trees dropping of leaves also affects this rate. Turnover rate of stored leaf pool and storage respiration depends on *storage turnover rate*, size of stored leaf pool, and storage biomass.
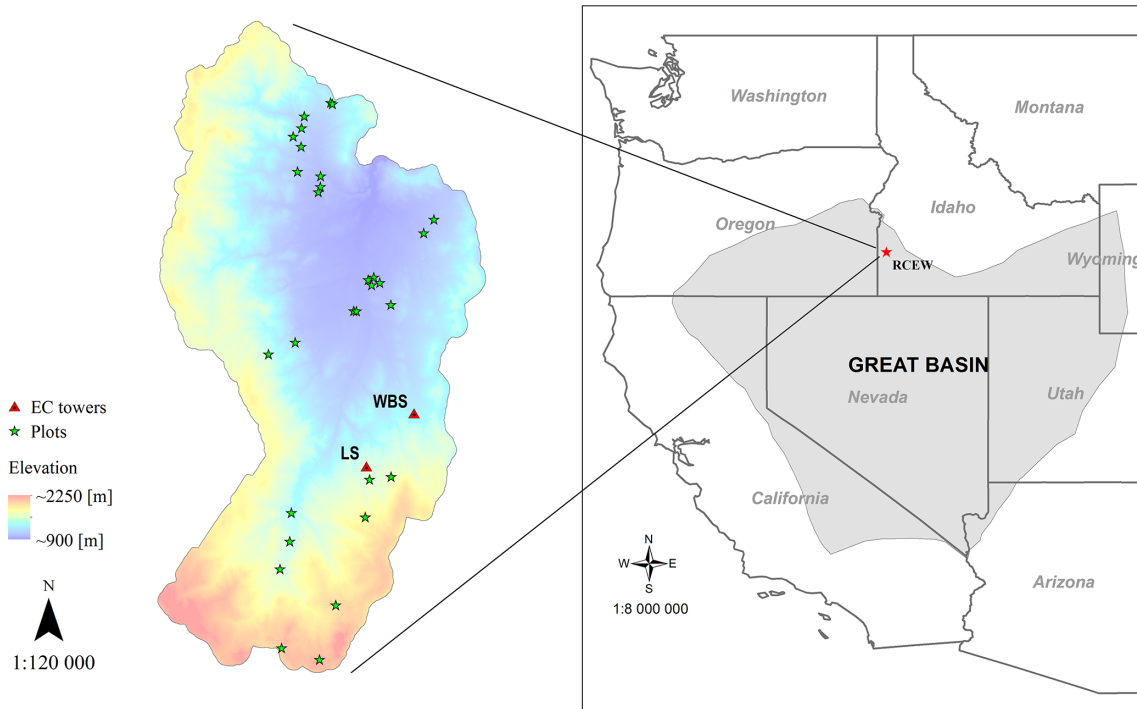
2.2 Study area

While the PFT was developed broadly for sagebrush, we developed the EDv2.2 model runs focused on the Reynolds Creek Experimental Watershed (RCEW), located in the northern Great Basin region of western United States (Fig. 1). The RCEW is operated by the USDA Agricultural Research Service and is also a Critical Zone Observatory (CZO) (referred to as RC-CZO). We used two 200 m × 200 m polygons centered at two EC sites within RC-CZO to closely represent the footprint area of these sites. The AmeriFlux US-Rls EC station, located at 43.1439° N, 116.7356° W and at an elevation of 1583 m, is within the Lower Sheep Creek

drainage in RCEW. The footprint of this site is dominated by low sagebrush (*Artemisia arbuscula*) and Sandberg bluegrass (*Poa secunda*) (Stephenson, 1970; Seyfried et al., 2000) and is characterized as having light cattle grazing (AmeriFlux, 2018). The second AmeriFlux tower, US-Rws, is located at 43.1675° N, 116.7132° W in the Nancy Gulch drainage, about 2 km northeast of the US-Rls site. This area is dominated by Wyoming big sagebrush (*A. tridentata* ssp. *wyomingensis*) and bluebunch wheatgrass (*Pseudoroegneria spicata*) (Stephenson, 1970). Hereafter, these two sites are designated as LS (for low sagebrush) and WBS (for Wyoming big sagebrush).

2.3 Inventory and EC tower data

A field inventory dataset of sagebrush shrubs from RCEW recorded in 2014 (Glenn et al., 2017) was used to fit the allometric equations (for temperate PFTs) in EDv2.2 and to initialize the ecosystem structure for the model simulations. Variables used to fit allometric equations for the sagebrush included volume, crown diameter, height, and stem diameter. EDv2.2 was originally developed for tropical forests, and thus typically specifies allometric relationships in terms of diameter at breast height (DBH). However, this length-scale variable has limited application to shrubs of the sagebrush-steppe ecosystem, which rarely exceed 1.5 m in height. Thus, we developed a substitute length-scale variable for DBH that effectively corresponds to shrub volume. To accomplish this, shrub volume was first calculated using crown area (characterized as an ellipse and approximated with semimajor and semiminor axis lengths) and height, and the cube root of this volume was then used as the characteristic length-scale variable required to parameterize allometric relationships in EDv2.2. To test this relationship, we compared height predicted from cube root volume with observed sagebrush height using a different set of data from the eastern side of the Sierra Nevada mountains, CA, in the Great Basin (Qi et al., 2018). We found a good fit for the data ($r^2 = 0.71$) with a small negative bias of -1.88 cm and a random residual distribution (Fig. S1). Using our field inventory from RCEW, we identified the coefficients in allometric equations (Table 2)

Figure 1. Location of EC flux sites in the RCEW study area: designated as LS (for low sagebrush) and WBS (for Wyoming big sagebrush). Field plots depicted were used to develop the allometric equations. The inset map shows the location of the RCEW study area within the northern Great Basin (LCC, 2018).

Table 3. Meteorological forcing data from the Weather Research and Forecasting (WRF) model used for simulation.

Variable	WRF name	Unit
Temperature at 2 m	T2	K
Surface pressure	PSFC	Pa
Accumulated precipitation	RAINNC	mm
Terrain height	HGT	m
U wind (zonal) component at 10 m	U10	$\mathrm{m\,s^{-1}}$
V wind (meridional) component at 10 m	V10	$\mathrm{m\,s^{-1}}$
Specific humidity at 2 m	Q2	$\mathrm{kg\,kg^{-1}}$
Downward longwave flux at ground surface	GLW	$\mathrm{W\,m^{-2}}$
Downward shortwave flux at ground surface	SWDOWN	$\mathrm{W\,m^{-2}}$

for shrub height, leaf biomass, structural biomass, canopy area, and wood area index as a function of this cube root of volume measure (used as DBH in the equation).

GPP data from 2015 to 2017 water years were derived from the LS and WBS EC stations (Fellows et al., 2017) using the REddyProc software in R (Reichstein et al., 2005) to fill and partition net ecosystem exchange (NEE) into ecosystem respiration and GPP.

2.4 Meteorological forcing data

Outputs from a long-term high-resolution climate reanalysis obtained from the Weather Research and Forecasting (WRF) model (Skamarock et al., 2008) were used to provide meteorological forcing data for the EDv2.2 model (Table 3). The WRF outputs correspond to atmospheric temperature and specific humidity at 2 m height, wind speed at 10 m height, downward shortwave radiation and longwave radiation at ground surface, surface pressure, and accumulated precipitation (Flores, et al., 2016). The spatial and temporal resolutions of the data are 1 km and 1 h, respectively. The EDv2.2 model then partitions shortwave radiation into direct and diffuse as well as visible and near-infrared components as summarized by Weiss and Norman (1985). We obtained these forcing data from 2001 to 2017 for two WRF pixels that spatially bound the LS and WBS sites (Fig. 1).

2.5 Initial parameterization and sensitivity analysis

We identified initial sagebrush shrub PFT parameters based on field allometric equations, previous research studies on the sagebrush ecosystem (Ahrends et al., 2009; Cleary et al., 2010; Comstock and Ehleringer, 1992; Gill and Jackson, 2000; Li et al., 2009; Olsoy et al., 2016; Qi et al., 2014; Sturges, 1977; Tabler, 1964), and information from other general PFT parameters in EDv2.2 (Table S1 in the Supple-

ment). The initial ecosystem states for the model run for the LS and WBS sites were designated to be a single sagebrush with 1 plant per square meter representing the average spacing from the 2014 field inventory data. For the LS site, we used 0.57 m of cube root volume (diameter) and 0.56 m for height and for WBS we used 0.62 m of cube root volume and 0.63 m for height. The soil column was configured to be 2.3 m deep with nine vertical layers and a free-drainage lower boundary. Corresponding to a gravelly loam soil in the study site (USDA, 2018a), we used a soil texture with 55 % sand, 25 % silt, and 20 % clay for both sites. Initial soil moisture was set to near saturation with no temperature offset, and the initial atmospheric carbon dioxide level matching the year 2001 (370 ppm), when we initialized the simulation. We ran the EDv2.2 model with these initial settings and initial shrub PFT parameters for the sensitivity analysis at the LS site for a 15-year simulation period. We selected this simulation period based on our pre-sensitivity trial runs, previous studies (Medvigy and Moorcroft, 2012; Antonarakis, et al., 2014) where authors had initialized models using inventory data, and taking into account that there have been no major disturbances in recent history at these sites. We used only one of our sites (LS site) for the sensitivity analysis because we assumed both sites are quite similar in terms of meteorological forcing (given their proximity) and ecosystem conditions, and particularly as we used a range of maximum and minimum values of parameters in the analysis.

Since our study focused preliminary on parameterization of the sagebrush PFT, we limited the sensitivity analysis to explore the linear dependence of selected parameters over target variables, assuming minimum nonlinear dependence among these parameters. We used a sensitivity index (SI) suggested by Hoffman and Gardner (1983) (Eq. 4) to perform a one-at-a-time sensitivity analysis and rank the parameters. Because this index is highly affected by the extreme values of parameters being studied, it is recommended that the parameter range cover the entire range of possible values. SI has been used in different areas of study including ecology (Waring et al., 2016) and hydrology (Wambura et al., 2015), mostly to assess the effect of parameters on target variables and sometimes to reduce the number of variables for further analysis.

$$SI = \frac{GPP_{max} - GPP_{min}}{GPP_{max}}, \tag{4}$$

where SI is sensitivity index, GPP_{max} is the value of GPP corresponding to the simulation with the maximum value of a parameter, and GPP_{min} is the value of GPP corresponding to the simulation with the minimum value of a parameter. We identified minimum and maximum possible values for each of the selected parameters based on previous sensitivity and optimization studies, the range of parameters for other PFTs in EDv2.2, and our preliminary sensitivity analyses (Table 4). EDv2.2 was then run for a 15-year period with both minimum and maximum values of each parame-

ter while keeping all other parameters constant. The average daily GPP outputs throughout the simulation years for maximum and minimum values of parameters were used to derive GPP_{max} and GPP_{min}, respectively. We limited the optimization to the five most sensitive parameters to keep time and computing performance manageable.

2.6 Optimization and validation

In the third step, optimization of the five selected parameters was performed for both the LS and WBS sites using an exhaustive search (brute-force) method within the specified range of values. This process was performed to identify the best values for the five selected parameters for each EC station in predicting GPP. A Bayesian method is often preferred in parameter optimization as it can assimilate multiple input data with a single model run and provide separate uncertainties for parameters, processes, and data. However, for a model like EDv2.2, it is nearly computationally prohibitive as we would need 10^4 to 10^7 model runs to perform associated Markov Chain Monte Carlo processes (Dietze et al., 2018; Fer et al., 2018). Likewise, there are model emulators (surrogate models) where statistical models are created to mimic full models by fitting parameters and response variables using distributions such as Gaussian. Experiments done with these model emulators are later transferred into the full model thus making this method computationally efficient. One of the drawbacks of this method is that it frequently fails to converge with nonlinear parameters (Fer et al., 2018; Keating et al., 2010). An alternative to these approaches is the brute-force method where all possible combinations of parameters from a uniform distribution within a predefined range are examined to get the best result. Advantages of the brute-force method are a higher possibility of identifying global optimums or fine tuning of posterior parameter ranges and assessing nonlinearity among parameters. The major disadvantage of this method is the computational cost but this can be reduced significantly by limiting the range of the parameter domain (Fer et al., 2018; Schmidtlein et al., 2010).

For each site, we ran 720 simulations with a unique combination of parameter values for 15 years (2001–2016), at which point it was assumed to reach an equilibrium with climate. EDv2.2 simulations were configured to allow for growth of the C_3 grass, northern pines, and late conifers together with the shrub PFT. This was done because although the vegetation assemblages in the flux site footprints are primarily composed of sagebrush and grasses, conifers are present in some parts of the experimental watershed (Seyfried et al., 2000). For each simulation, we calculated a skill score, Nash–Sutcliffe efficiency (NSE) (Nash and Sutcliffe, 1970), to compare the simulated GPP from 2015 and 2016 with those derived from LS and WBS EC stations for respective years. Although, NSE is closely related to root mean square error (RMSE) (or mean square error, MSE), the
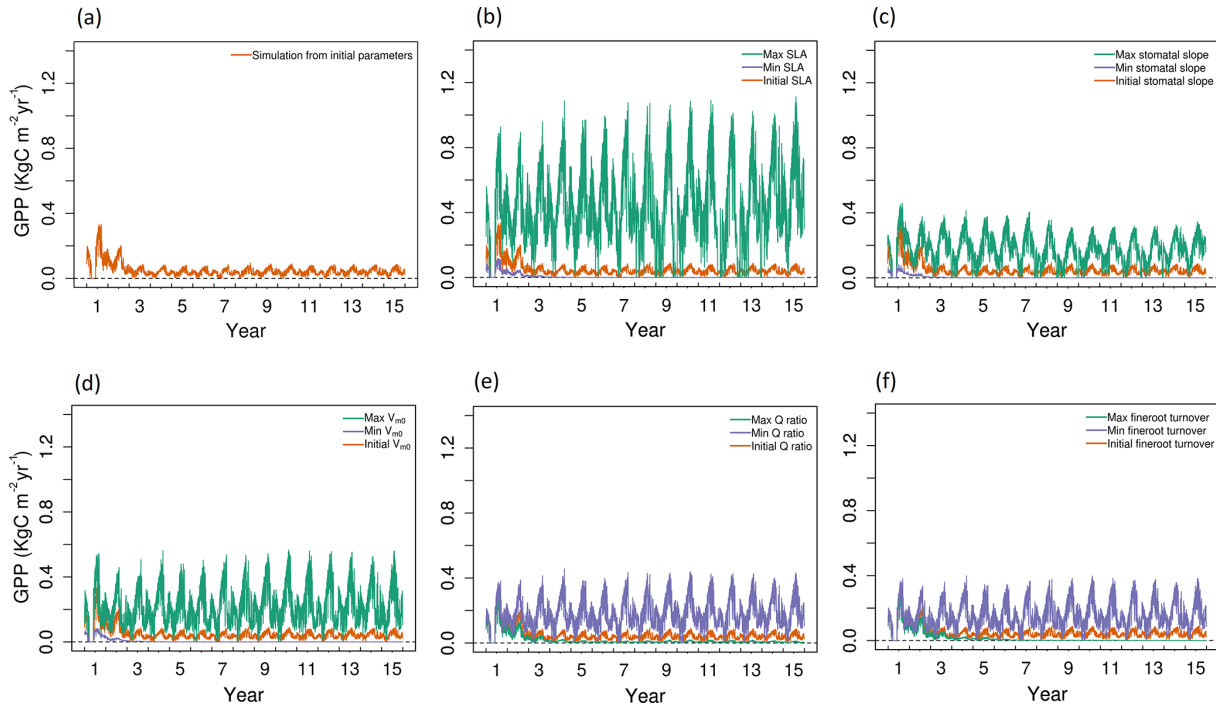
Figure 2. Simulated daily GPP outputs from 1 to 15 years for the study location with **(a)** initial values of all five parameters and **(b–f)** maximum (green), minimum (blue), and initial (red) parameter values for SLA, stomatal slope, $V_{m,0}$, Q ratio, and fine root turnover rate.

skill score from it can be interpreted as comparative ability of the model over a baseline model, which is the mean of site observations in this case. While the RMSE value depends on the unit of predicted variables, which can vary from 0 to infinity, the NSE is dimensionless and varies from negative infinity to 1 (Krause et al., 2005; Gupta et al., 2009). NSE is calculated using Eq. (5):

$$\text{NSE} = 1 - \frac{\sum_{i=1}^{n} (O_i - P_i)^2}{\sum_{i=1}^{n} (O_i - \underline{O})^2}, \tag{5}$$

where O_i is observation, P_i is predicted value, $\underline{O}$ is mean of observation, and n is number of observations. For both EC stations, we selected the 10 best simulations based on NSE scores, computed ensemble means of all five parameter values, and estimated mean GPP. Outputs from process-based models like EDv2.2 are often ill-posed outputs, meaning that there may not be a unique solution of parameter combinations but rather several combinations of parameters produce the same solution. One way to solve the ill-posed problem is by selecting more than one of the best combinations, from which we can either explore average outputs or select one of the ensemble members that would better match any prior information such as any correlation among parameters, available data, vegetation characteristics, or ecosystem conditions (Combal et al., 2002; Quan et al., 2015). The simulated GPP from these runs were then compared against respective EC

site data from 2017, which was withheld from the optimization as a means of providing an independent validation.

3 Results

3.1 Initial parameterization and sensitivity analysis

For the model run based on the initial values of parameters (Table S1 of the Supplement), the 15-year simulations produced an annual cycle in GPP that decreases in amplitude during the initial 1–3 years, and remains at a level of approximately $0.07 \, \text{kg C m}^{-2} \, \text{yr}^{-1}$ in the remaining years (Fig. 2a). Observed GPP values in 2016 were $0.51 \, \text{kg C m}^{-2} \, \text{yr}^{-1}$ and $0.38 \, \text{kg C m}^{-2} \, \text{yr}^{-1}$ for the LS and WBS sites, respectively. This result was significantly lower than the observed GPP from either of the EC sites, and thus we followed up with sensitivity and optimization analyses to constrain some of the influential parameters.

Based on the SI ranking, SLA, stomatal slope, V_{m0}, fine root turnover rate, and Q ratio were identified as the top five sensitive parameters compared to the other parameters explored (Fig. 2; Table 4). Related studies (Dietze et al., 2014; Medvigy et al., 2009; Pereira et al., 2017; Zaehle et al., 2005) have also identified similar model parameters being important in estimating GPP. In our study, higher parameter values of SLA, stomatal slope, and V_{m0}, resulted in higher GPP estimates (Fig. 2b, c, and d), whereas for Q ratio and fine root

Table 4. Summary of sensitivity analysis of studied PFT parameters ranked by sensitivity index (SI).

Parameters	Initial	Min	Max	SI	Reference
SLA ($m^2 kg^{-1}$)	4.5	2	15	0.988	Lambrecht et al. (2007); Brabec (2014); Olsoy et al. (2016)
Stomatal slope	7	2	15	0.983	Dietze et al. (2014); Bonan et al. (2014)
V_{m0} ($\mu mol\,m^{-2}\,s^{-1}$)	16.5	4	30	0.982	Comstock and Ehlenger (1992); Oleson et al. (2013)
Q ratio	3.2	0.4	12	0.898	Dietze et al. (2014)
Fine root turnover rate (a^{-1})	0.33	0.1	2	0.895	Gill and Jackson (2000)
Cuticular conductance ($\mu mol\,m^{-2}\,s^{-1}$)	10^3	10^2	10^7	0.813	Barnard and Bauerle (2013); Duursma et al. (2019)
Leaf turnover rate (a^{-1})	1	0.1	2	0.779	*
GRF	0.33	0.11	0.66	0.694	Wang et al. (2013)
Water conductance ($ms^{-1}\,kg\,C$ per root)	1.9×10^{-5}	1.9×10^{-6}	1.9×10^{-4}	0.168	*
Storage turnover rate (a^{-1})	0.624	0.33	0.95	0.004	*
Leaf width (m)	0.05	0.01	0.10	0.002	*

* Information about the range comes from range of values for other PFTs in EDv2.2, and our preliminary sensitivity analysis.

turnover rate higher parameter values produced lower GPP (Fig. 2e and f). The impact of shifts in SLA, V_{m0}, and stomatal slope values are observed from the very beginning of the simulations, while changes in fine root turnover rate and Q-ratio parameters start to show differences from roughly 3–4 years after the initial model run. Although not ranked in the top five, cuticular conductance, leaf turnover rate, and growth respiration factor also had considerable influences over GPP (Table 4).

3.2 Optimization and validation

For our exhaustive search of parameter values, we limited search domains for parameters based on previous studies and the result of our sensitivity analysis. SLA search limits were largely based on Olsoy et al. (2016), who suggested a range of 3 to 6 $m^2 kg^{-1}$ for sagebrush SLA, with regional and seasonal variations. Similarly, limits for V_{m0} were extended slightly beyond the recommendations by Comstock and Ehleringer (1992) for the Great Basin shrubs, and the upper limit for stomatal slope was extended slightly beyond that used by Oleson et al. (2013) for a shrub PFT in the Community Land Model (CLMv4.5). We set search domains for Q ratio based on a leaf and root biomass study of sagebrush by Cleary et al. (2010), and fine root turnover ratio was based on results from a study on *Artemisia ordosica* in a semiarid region of China (Li et al., 2009). Interval distances (or "steps") were calculated to equally space out the range between the maximum and minimum of each parameter for a given number of intervals (Table 5). Parameters identified as exerting more control on GPP prediction were assigned a higher number of steps, resulting in the following: five steps for SLA, four steps for V_{m0}, and stomatal slope, and three steps for Q ratio and fine root turnover rate. Among 720 possible simulations for unique parameter value combinations for each site,

Table 5. Minimum value, maximum value, interval size, and number of steps for each parameter used in optimization.

| Parameter	Min	Max	Interval	Number of steps
SLA ($m^2 kg^{-1}$)	3.00	9.00	1.50	5
V_{m0} ($\mu mol\,m^{-2}\,s^{-1}$)	14.00	21.50	2.50	4
Stomatal slope	7.00	10.00	1.00	4
Fine root turnover (a^{-1})	0.11	0.33	0.11	3
Q ratio	0.40	3.20	1.40	3

92 cases from LS and 116 cases from WBS, which did not provide model optimization results because of numerical instabilities (with GPP approaching zero), were excluded from subsequent analysis.

We selected 10 simulations with the best NSE scores for both the LS and WBS sites (Table S2 and Fig. S1 in the Supplement) and determined ensemble means of parameter values for these sites (Table 6). To perform validation of these 10 best simulations from each EC station, we extended the model runs to obtain GPP estimates for the year 2017. We then compared the biases and skill scores associated with the top-performing simulation (hereafter the "best case") and the mean from all 10 simulations (hereafter the "ensemble mean"). Among the 10 best simulations selected for each EC site, 4 of them were common to both sites (Table S2 in the Supplement). We observed that the variation in parameter values was more pronounced for the LS site, especially with regard to V_{m0} and stomatal slope. Likewise, we identified more variation in GPP estimates among 10 best simulations for LS site than for WBS site, especially during the peak and trough periods in the plots (Fig. S2 in the Supplement).

Table 6. Optimized parameter values from best cases and top 10 ensembles (mean and standard deviation (SD)) for LS and WBS EC stations.

Parameters	LS EC station		WBS EC station	
	Best case	Ensemble mean and SD	Best case	Ensemble mean and SD
V_{m0} (μmol m^{-2} s^{-1})	19.00	19.00 ± 1.66	19.00	18.25 ± 1.21
SLA (m^2 kg^{-1})	7.50	8.10 ± 0.77	7.50	8.10 ± 0.77
Stomatal slope	9.00	8.70 ± 0.94	9.00	9.10 ± 0.32
Fine root turnover (a^{-1})	0.22	0.19 ± 0.09	0.33	0.23 ± 0.08
Q ratio	3.20	2.08 ± 1.29	1.80	1.80 ± 1.14
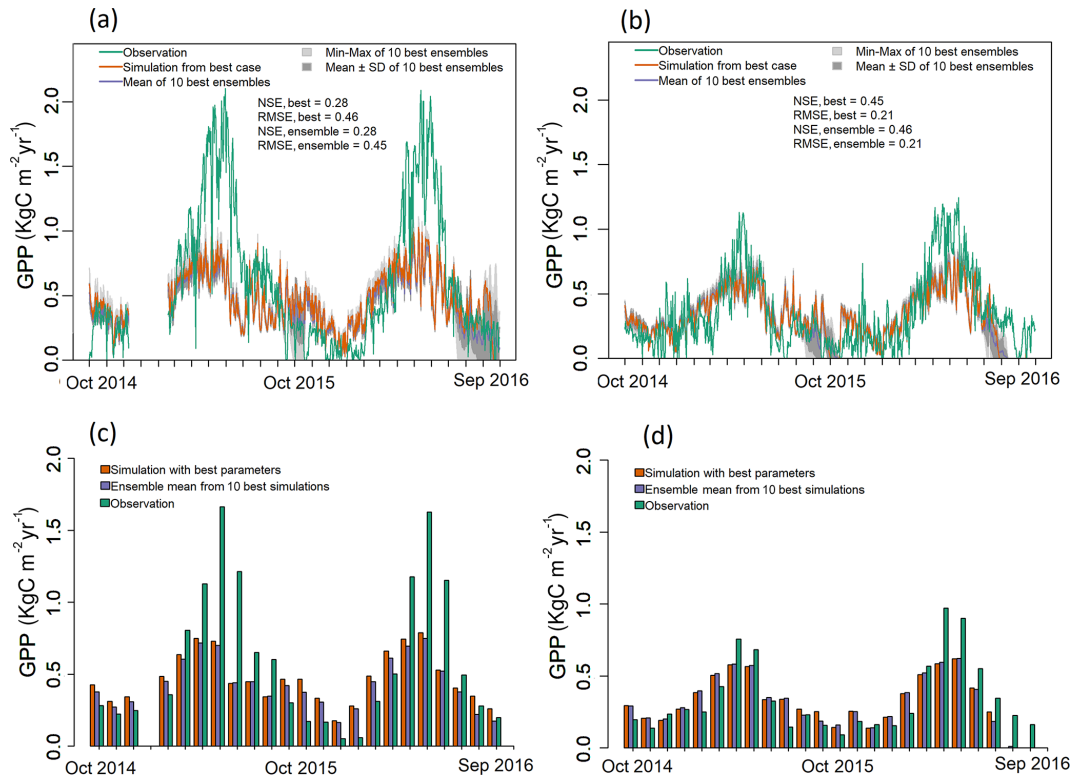
Figure 3. Observed and simulated GPP for the optimization period (water years 2015 and 2016) for both EC towers. **(a–b)** Simulated daily GPP (kg C m^{-2} yr^{-1}) from best case, 1 standard deviation of ensembles, and range of ensemble simulations compared with observations for **(a)** LS and **(b)** WBS sites. **(c–d)** Simulated mean monthly GPP (kg C m^{-2} yr^{-1}) from best case and ensemble means compared against observation data for **(c)** LS and **(d)** WBS sites. Note that observation data from 11 December 2014 to 17 February 2015 are missing for LS site.

The best case for WBS site showed traces of C$_3$ grass growth through some intermediate simulation years even though we initialized the model with only the shrub PFT (Fig. S3 in the Supplement). Optimized parameter values were only slightly different between the best case and ensemble means for both sites, possibly suggesting little interaction effects among the parameters (Table 6). In the best case, parameter values for V_{m0}, SLA, and stomatal slope were the same for both sites, whereas Q ratio and fine root turnover rate were different. We also observed that fine root turnover rate and Q ratio had higher variability among the 10 best simulations compared to the rest of the parameters for both sites. Our comparison

of variation between the two sites among ensemble members showed that the WBS site had overall lower variation than the LS site (Table 6), and V_{m0} had noticeably lower variation for the WBS site.

Figure 3 presents simulated GPP from the best case, variation among 10 best ensemble members, and ensemble mean for the final two model years (October 2014 to September 2016) along with the observed GPP from the same period from each EC station. Optimization results for the LS site in Fig. 3a show that simulated GPP matches well with observed data for most days, except during the spring season, during which strong peaks in observed GPP were not

Table 7. Bias, NSE, and RMSE for optimization and validation of GPP for the best case and the top 10 ensemble means for both EC stations.

Simulations	Optimization			Validation		
	Bias ($\mathrm{kg\,C\,m^{-2}\,yr^{-1}}$)	NSE	RMSE ($\mathrm{kg\,C\,m^{-2}\,yr^{-1}}$)	Bias ($\mathrm{kg\,C\,m^{-2}\,yr^{-1}}$)	NSE	RMSE ($\mathrm{kg\,C\,m^{-2}\,yr^{-1}}$)
LS						
Best case	−0.137	0.277	0.456	−0.257	0.069	0.554
Ensemble mean	−0.172	0.281	0.455	−0.278	0.053	0.559
WBS						
Best case	−0.028	0.452	0.213	−0.252	0.079	0.411
Ensemble mean	−0.030	0.456	0.212	−0.265	0.036	0.420

captured by the simulation results. Average monthly comparisons (Fig. 3c) show that simulated GPPs are close to the observations for most of the months except for April, May, and June, during which the model is clearly underestimating GPP. We observed a small variation (Fig. 3a) among 10 ensemble simulations with an average standard deviation of $0.057\,\mathrm{kg\,C\,m^{-2}\,yr^{-1}}$, where most of the variations were observed during fall and early spring. Variations during fall months are evident in the monthly average GPP, in which there was often considerable difference between ensemble mean and best case estimations for September and October (Fig. 3c and d). Despite GPP estimation from ensemble mean ($-0.17\,\mathrm{kg\,C\,m^{-2}\,yr^{-1}}$) having higher negative bias compared to the best case ($-0.14\,\mathrm{kg\,C\,m^{-2}\,yr^{-1}}$), its skill score (NSE) was marginally higher (Table 7). In comparison to the LS site, the WBS site had lower spring peaks in GPP, which were also limited to fewer months (Fig. 3b and d) and were far more comparable to the simulation results. The average standard deviation among ensemble simulations ($0.037\,\mathrm{kg\,C\,m^{-2}\,yr^{-1}}$) was lower for WBS than for LS, resulting in little difference between best case and ensemble mean estimations for that site. Both the WBS and LS ensemble mean simulations produced only a marginally higher NSE than the best case results. However, the spring mismatch in the LS site resulted in higher Bias and lower NSE when compared to the WBS site (Table 7). Yet, despite negative biases during spring, positive NSE scores for both sites suggest that the parameters were generally functioning to allow the model to track observed daily GPP over time.

For validation of the parameter estimates, we ran the EDv2.2 model for all 10 best simulations with corresponding parameter values from 2016 to 2017 for both the LS and WBS sites and compared the simulated GPPs from the 2017 water year with observed GPP from the respective locations in the same year. Results from the model validation showed greater negative biases and lower NSEs for both sites compared to the optimization results (Table 7). Moreover, there were substantial differences in mean GPP observations from EC sites for both LS and WBS

sites, between optimization ($\mathrm{LS}=0.61\,\mathrm{kg\,C\,m^{-2}\,yr^{-1}}$, $\mathrm{WBS}=0.35\,\mathrm{kg\,C\,m^{-2}\,yr^{-1}}$) and validation ($\mathrm{LS}=0.55\,\mathrm{kg\,C\,m^{-2}\,yr^{-1}}$, $\mathrm{WBS}=0.46\,\mathrm{kg\,C\,m^{-2}\,yr^{-1}}$) years. Validation results were slightly better for the WBS than the LS site; however, the difference in validation performance among the two sites was not as distinct as with the optimization results. Overall, positive NSE values for both cases (best case and ensemble mean) for both sites suggest that the simulated estimates provided better GPP predictions than the observed means. Poor validation results could be attributed to interannual variability in observed GPPs and to the inability of the model to adequately capture peak spring growth.

Validation results shown in Fig. 4 also indicate that the simulated daily GPPs for both sites matched observed values relatively well from late fall until early spring months (October–April) but performed poorly in the late spring and summer months (May–September) when compared with observation data from 2017. Daily patterns of simulated GPP were almost identical for both sites, with GPP falling sharply through late summer months and remaining close to zero. Observed GPP data values at both sites showed similar patterns of decline in 2017 during late summer months (July and August), though not as sharply as the simulated results (Fig. 4). The observed increase in GPP at the beginning of fall (September) was not well captured by the simulated outputs for either site. Monthly averages also clearly show differences between simulated and observed GPP for May through September (Fig. 4c, d). Variation among ensemble simulations was higher for the LS site compared to the WBS site, with standard deviations of 0.056 and $0.02\,\mathrm{kg\,C\,m^{-2}\,yr^{-1}}$, respectively. When validation and optimization results are compared, the variation between the ensemble simulations of the LS site were relatively similar, whereas ensemble variation was generally lower in the validation output for the WBS site. Ensemble means for both sites for validation exhibited almost identical patterns as the best case simulations, though at slightly lower levels for most of the months.
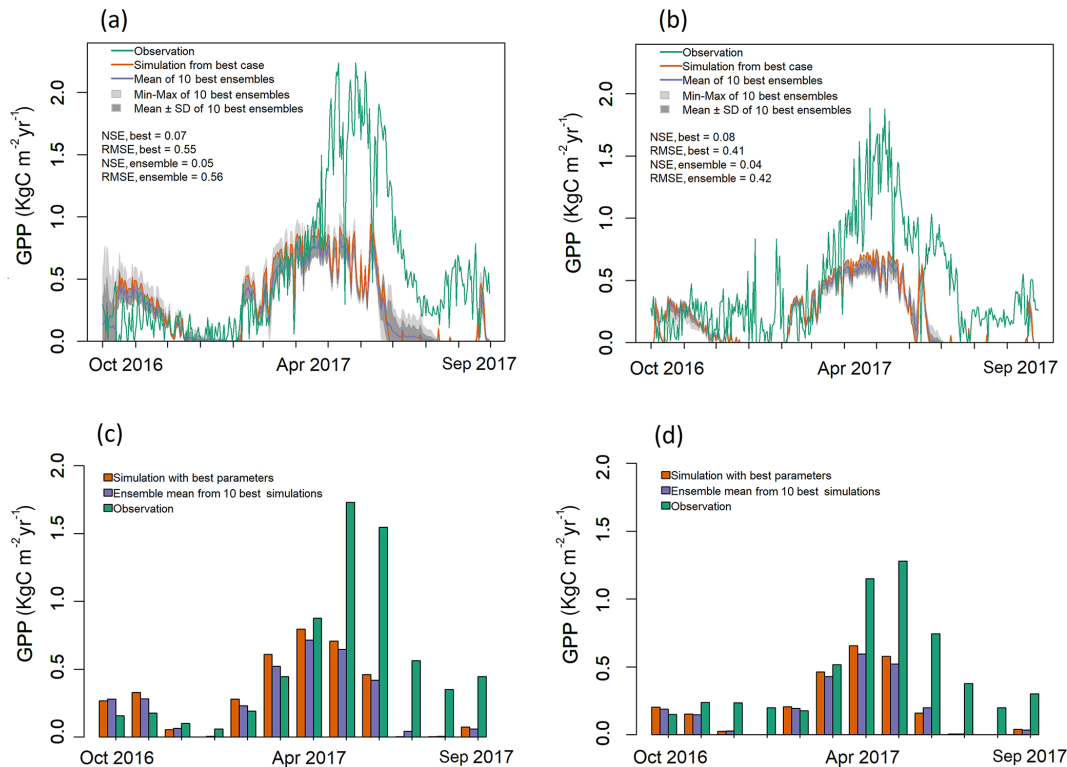
Figure 4. Observed and simulated GPP for validation period (water year 2017) for both EC towers. **(a–b)** Simulated daily GPP (kg C m^{-2} yr^{-1}) from best case, 1 standard deviation of ensembles, and range of ensemble simulations compared with observations for **(a)** LS and **(b)** WBS sites. **(c–d)** Simulated mean monthly GPP (kg C m^{-2} yr^{-1}) from best case and ensemble means compared against observation data for **(c)** LS and **(d)** WBS sites.

4 Discussion

Using our newly developed sagebrush shrub PFT, we were able to effectively simulate sagebrush ecosystem productivity in EDv2.2 as represented by the two study sites. Simulated results, after about 4 modeled years, clearly maintained annual shrub GPP over time, although at a lower level than the observed data from these sites. To improve GPP estimates and reduce uncertainty, we assessed the sensitivity of 11 different parameters closely associated with biomass growth. Results from this preliminary analysis were similar to previous studies (Dietze et al., 2014; LeBauer et al., 2013; Medvigy et al., 2009), wherein parameters V_{m0}, SLA, fine root turnover rate, and stomatal slope were found to be the most influential in determining carbon flux or primary productivity. We observed variation in these parameter values for 10 best simulations selected based on NSE values (Table S2 in the Supplement) for both sites where the LS site had higher variation in V_{m0} and stomatal slope than the WBS site. The effects of some parameters (stomatal slope, fine root turnover rate, and Q ratio) on GPP prediction differed when they were altered individually versus simultaneously with other parameters. For instance, sensitivity analysis suggested GPP increases when fine root turnover ratio and Q ratio are lower-

ered individually, yet the best results for each site did not improve (i.e., still underpredicted GPP) with the lowest values of these parameters. Indeed, in addition to 1st-order effects of the studied parameters, the top 10 best parameter combinations exhibited variation in parameter values for both EC sites, suggesting interacting effects and potential nonlinear dependence among parameters. The best case parameters identified from the optimization suggested some difference in fine root turnover rate and Q ratio between the LS and WBS sites. We found a similar pattern of marginally higher fine root turnover rate and lower Q ratio at WBS with the ensemble mean, despite substantial variation among the 10 ensemble members. We can potentially relate these differences in parameters between the LS and WBS sites with differences in the root systems and vegetation height of low sagebrush and Wyoming big sagebrush species, which are the dominant vegetation types of the respective sites. Low sagebrush is a smaller plant with primarily a shallow fibrous root system, whereas Wyoming big sagebrush is taller with a dual taproot and shallow-root system (Steinberg, 2002; USDA, 2018b).

Negative bias in estimated GPP for the best simulations resulted from an inability of the model to correctly produce daily GPPs for late spring and summer months. Although a higher annual GPP could be obtained to compensate for neg-

ative bias by changing parameter values, the highest GPP was not necessarily the one with the best NSE since NSE was calculated based on daily GPP values. Limiting optimization to 5 of the 11 parameters initially identified may have also contributed to the error and bias observed in our modeled estimates. Our generalization of shrubland ecosystem processes (as trees in the EDv2.2 model structure) may also be one of the limiting factors. Open and scattered shrubland ecosystems as in our study area (Mitchell et al., 2011) do not follow the same pattern of recruitment and competition as we would expect for a closed canopy ecosystem (Schwantes et al., 2016; Wolf et al., 2008). In addition, future studies should give special consideration to phenology, seed dispersal, and mortality that are unique to these shrubland ecosystems. Even though the PFT parameters and allometric coefficients that we developed for shrub PFT influence the abovementioned ecosystem processes, we suggest modification of some of these model structures in future studies to test their influence and potentially improve GPP estimates.

GPP simulations for the WBS site had better optimization scores than for the LS site, and also a slight edge over the latter for validation results. This could be due to differences in soils and hydraulic conditions between the sites as we used similar setups for our simulation. Moreover, variation between morphological characteristics of the vegetation at the LS and WBS EC towers (characterized by low sagebrush and Wyoming big sagebrush, respectively), including growing seasons and flowering seasons, may also have resulted in the observed differences in GPP (Howard, 1999; USDA, 2018b). Since Wyoming big sagebrush is the dominant species in the Reynolds Creek Experimental Watershed area (Seyfried et al., 2000), the allometric equations fitted for sagebrush (representing most areas of RCEW) could favor the more realistic growth pattern of this species in the model (e.g., Figs. 3 and 4).

Additionally, differences in the phenology of the associated grass species between the two sites could result in differences in seasonal and annual productivity (Cleary et al., 2015). For instance, the perennial grass at the LS site is Sandberg bluegrass, which is photosynthetically active in early spring and senesces by early summer (USDA, 2016), and thus may have contributed to the observed higher spring GPP peak at the LS site. Although, we observed small amounts of simulated GPP growth for C_3 grasses for certain intermediate years, these levels were not sustained. However, current parameters for C_3 grasses were unlikely to adequately produce coexistence of grasses in the area, and we could not validate results in terms of the actual species composition and ecosystem dynamics of the EC sites as we did not have GPP observations for unique PFTs. We also observed high interannual variation in observed GPP for both sites, leading to poor results in validation of simulation outputs. In summary, site-specific variability, model complexity, and optimizing for only five parameters likely contributed to, or

were responsible for, the differences between modeled and observed GPP estimates.

While the emphasis of this study was to develop and optimize the shrub PFT parameters, we expect that simultaneous optimization of both grass and shrub PFTs would result in improved representation of the vegetation composition in the study area. Such an effort would also increase the number of parameters required, potentially complicating the process of optimization and validation unique to each PFT. Moreover, several studies suggest that the parameters V_{m0} and SLA vary considerably across seasons (Groenendijk et al., 2011; Kwon et al., 2016; Olsoy et al., 2016; Zhang et al., 2014). The mismatch in daily GPP patterns between simulated and flux tower data for specific seasons could be partly attributed to the lack of the model's ability to address these seasonal deviations correctly. Like most other terrestrial biosphere models, EDv2.2 does not incorporate seasonal variation in V_{m0}, SLA, or other model parameters (Medvigy et al., 2009).

The optimization scheme implemented in our study has some limitations. For example, we assumed the distribution of all parameters of interest to be uniform but this may not be true. Similarly, to keep computational time practical, we excluded some of the sensitive parameters such as cuticular conductance, leaf turnover rate, and GRF from the optimization analysis. We may achieve better results in parameter optimization and GPP estimates by making advances in our methods in future studies. For example, we can utilize additional sensitivity (including variance decomposition and 1st- and 2nd-order analyses) (Zhang et al., 2017) and optimization (including cost function, gradient descent, and uncertainty analysis) (Richardson et al., 2010) methods to fine-tune the sagebrush PFT parameters. Similarly, if we include additional years of observation data, we may better capture interannual variability normally observed in ecosystem fluxes, and potentially improve validation outcomes.

5 Conclusions

This study demonstrates that despite the complexity of the sagebrush-steppe ecosystem, estimating GPP using the newly developed sagebrush PFT is comparable, although with seasonal bias, to observations obtained from EC station sites. Since our primary focus here was to develop initial parameters (including allometric relationships) for the shrub (sagebrush) PFT in EDv2.2, we focused our efforts on utilizing simple sensitivity and optimization tools to constrain errors associated with simulated GPP. Our identification of coefficients for allometric equations coupled with the other parameters for the semiarid shrub PFT for EDv2.2 will permit exploration of additional research questions. For instance, EDv2.2 could be run at regional scales with optimized parameters to model the spatiotemporal dynamics of the sagebrush community composition and ecosystem flux under different climate and ecological restoration scenarios. PFT pa-

rameters identified and constrained from this study can be used as preliminary prior information in future studies related to sagebrush. We can either use the best case parameter sets from one of the study sites, depending upon the dominant sagebrush type, or we can use any 1 of the 10 ensemble parameters if we have reliable information on the studied parameters. With additional time and computing resources (to facilitate large numbers of simulations), we can further refine sagebrush parameters to explore variance decomposition and nonlinear dependencies using different sensitivity and optimization methods. Optimization of associated or co-occurring PFTs (C_3 grass and conifers) in the region, spanning out to include additional study sites, would also help to better understand and constrain uncertainties in estimating the complex dynamics of the sagebrush-steppe ecosystem.

References

Ahrends, H. E., Etzold, S., Kutsch, W. L., Stockli, R., Bruegger, R., Jeanneret, F., Wanner, H., Buchmann, N., and Eugster, W.: Tree phenology and carbon dioxide fluxes: use of digital photography for process-based interpretation of the ecosystem scale, Clim. Res., 39, 261–274, 2009.

AmeriFlux: http://ameriflux.lbl.gov, last access: 7 May 2018.

Antonarakis, A. S., Munger, J. W., and Moorcroft, P. R.: Imaging spectroscopy- and lidar-derived estimates of canopy composition and structure to improve predictions of forest carbon fluxes and ecosystem dynamics, Geophys. Res. Lett., 41, 2535–2542, https://doi.org/10.1002/2013GL058373, 2014.

Barnard, D. M. and Bauerle, W. L.: The implications of minimum stomatal conductance on modeling water flux in forest canopies, J. Geophys. Res.-Biogeo., 118, 1322–1333, https://doi.org/10.1002/jgrg.20112, 2013.

Bonan, G. B., Williams, M., Fisher, R. A., and Oleson, K. W.: Modeling stomatal conductance in the earth system: linking leaf water-use efficiency and water transport along the soil–plant–atmosphere continuum, Geosci. Model Dev., 7, 2193–2222, https://doi.org/10.5194/gmd-7-2193-2014, 2014.

Bond-Lamberty, B., Fisk, J. P., Holm, J. A., Bailey, V., Bohrer, G., and Gough, C. M.: Moderate forest disturbance as a stringent test for gap and big-leaf models, Biogeosciences, 12, 513–526, https://doi.org/10.5194/bg-12-513-2015, 2015.

Botkin, D. B., Janak, J. F., and Wallis, J. R.: Rationale, Limitations, and Assumptions of a Northeastern Forest Growth Simulator, IBM J. Res. Dev., 16, 101–116, 1972.

Brabec, M. M.: Big Sagebrush (Artemisia tridentata) in a shifting climate context: assessment of seedling responses to climate, Master's Thesis, Boise State University, United States, 116 pp., 2014.

Bradley, B. A.: Assessing ecosystem threats from global and regional change: hierarchical modeling of risk to sagebrush ecosystems from climate change, land use and invasive species in Nevada, USA, Ecography, 33, 198–208, 2010.

Chambers, J. C., Miller, R. F., Board, D. I., Pyke, D. A., Roundy, B. A., Grace, J. B., Schupp, E. W., and Tausch, R. J.: Resilience and Resistance of Sagebrush Ecosystems: Implications for State and Transition Models and Management Treatments, Range

Ecol. Manage., 67, 440–454, https://doi.org/10.2111/REM-D-13-00074.1, 2014.

Cleary, M. B., Pendall, E., and Ewers, B. E.: Aboveground and belowground carbon pools after fire in mountain big sagebrush steppe, Range Ecol. Manage., 63, 187–96, https://doi.org/10.2111/REM-D-09-00117.1, 2010.

Cleary, M. B., Naithani, K. J., Ewers, B. E., and Pendall, E.: Up-scaling CO_2 fluxes using leaf, soil and chamber measurements across successional growth stages in a sagebrush steppe ecosystem, J. Arid Environ., 121, 43–51, 2015.

Combal, B., Baret, F., Weiss, M., Trubuil, A., Mace, D., Pragnere, A., Myneni, R., Knyazikhin, Y., and Wang, L.: Retrieval of canopy biophysical variables from bidirectional reflectance using prior information to solve the ill-posed inverse problem, Remote Sens. Environ., 84, 1–15, https://doi.org/10.1016/S0034-4257(02)00035-4, 2003.

Comstock, J. P. and Ehleringer, J. R.: Plant adaptation in the Great Basin and Colorado Plateau, Great Basin Nat., 52, 195–215, 1992.

Connelly, J. W., Knick, S. T., Schroeder, M. A., and Stiver, S. J.: Conservation Assessment of Greater Sage-grouse and Sagebrush Habitats, Western Association of Fish and Wildlife Agencies, Unpublished Report, Cheyenne, Wyoming, 2004.

Dietze, M. C., Serbin, S. P., Davidson, C., Desai, A. R., Fend, X., Kelly, R., Kooper, R, LeBauer, D., Mantooth, J., McHenry, K., and Wang, D.: A quantitative assessment of a terrestrial biospheremodel's data needs across North American biomes, J. Geophys. Res.-Biogeo., 119, 286–300, https://doi.org/10.1002/2013JG002392, 2014.

Dietze, M. C., Fox, A., Beck-Johnson, L. M., Betancourt, J. L., Hooten, M. B., Jarnevich, C. S., Keitt, T. H., Kenney, M. A., Laney, C. M., Larsen, L. G., Loescher, H. W., Lunch, C. K., Pijanowski, B. C., Randerson, J. T., Read, E. K., Tredennick, A. T., Vargas, R., Weathers, K. C., and White, E. P.: Iterative near-term ecological forecasting: Needs, opportunities, and challenges, P. Natl. Acad. Sci. USA, 115, 1424–1432, https://doi.org/10.1073/pnas.1710231115, 2018.

Duursma, R. A., Blackman, C. J., Lopez, R., Martin-StPaul, N. K., Cochard, H., and Medlyn, B. E.: On the minimum leaf conductance: its role in models of plant water use, and ecological and environmental controls, New Phytol., online version, 221, 693–705, https://doi.org/10.1111/nph.15395, 2019.

ED-2 model development team: Ecosystem Demography model (ED-2) code repository, available at: https://github.com/EDmodel/ED2 (last access: 20 September 2019), 2014.

Farquhar, G. D. and Sharkey T. D.: Stomatal conductance and photosynthesis, Ann. Rev. Plant Physiol., 33, 317–345, 1982.

Fellows, A. W., Flerchinger, G. N., Seyfried, M. S., and Lohse, K.: Data for Partitioned Carbon and Energy Fluxes Within the Reynolds Creek Critical Zone Observatory, Data set, https://doi.org/10.18122/B2TD7V, 2017.

Fer, I., Kelly, R., Moorcroft, P. R., Richardson, A. D., Cowdery, E. M., and Dietze, M. C.: Linking big models to big data: efficient ecosystem model calibration through Bayesian model emulation, Biogeosciences, 15, 5801–5830, https://doi.org/10.5194/bg-15-5801-2018, 2018.

Fisher, R., McDowell, N., Purves, D., Moorcroft, P., Sitch, S., Cox, P., Huntingford, C., Meir, P., and Woodward, F. I.: Assessing uncertainties in a second-generation dynamic vegetation model caused by ecological scale limitations, New Phytol., 187, 666–681, https://doi.org/10.1111/j.1469-8137.2010.03340.x, 2010.

Fisher, R. A., Koven, C. D., Anderegg, W. R. L, Christoffersen, B. O., Dietze, M. C., Farrior, C. E. Holm, J. A., Hurtt, G. C., Knox, R. G., Lawrence, P. J., Lichstein, J. W., Longo, M., Matheny, A. M., Medvigy, D., Muller-Landau, H. C., Powell, T. L., Serbin, S. P., Sato, H., Shuman, J. K., Smith, B., Trugman, A. T., Viskari, T., Verbeeck, H., Weng, E., Xu, C., Xu, X., Zhang, T., and Moorcroft, P. R.: Vegetation demographics in Earth System Models: A review of progress and priorities, Glob. Change Biol., 24, 35–24, https://doi.org/10.1111/gcb.13910, 2018.

Flores, A., Masarik, M., and Watson, K.: A 30-Year, Multi-Domain High-Resolution Climate Simulation Dataset for the Interior Pacific Northwest and Southern Idaho, data set, https://doi.org/10.18122/B2LEAFD001, 2016.

Gill, R. A. and Jackson, R. B.: Global patterns of root turnover for terrestrial ecosystems, New Phytol., 147, 13–31, doi.org/10.1046/j.1469-8137.2000.00681.x, 2000.

Glenn, N.F., Spaete, L. P., Shrestha, R., Li, A., Ilangakoon, N., Mitchell, J., Ustin, S. L., Qi, Y., Dashti, H., and Finan, K.: Shrubland Species Cover, Biometric, Carbon and Nitrogen Data, Southern Idaho, 2014, ORNL DAAC, Oak Ridge, Tennessee, USA, data set, https://doi.org/10.3334/ORNLDAAC/1503, 2017.

Groenendijk, M., Dolman, A. J., Ammann, C., Arneth, A., Cescatti, A., Dragoni, D., Gash, J. H. C., Gianelle, D., Gioli, B., Kiely, G., Knohl, A., Law, B. E., Lund, M., Marcolla, B., Van Der Molen, M. K., Montagnani, L., Moors, E., Richardson, A. D., Roupsard, O., Verbeeck, H., and Wohlfahrt, G. Seasonal variation of photosynthetic model parameters and leaf area index from global Fluxnet eddy covariance data, J. Geophys. Res., 116, G04027, https://doi.org/10.1029/2011JG001742, 2011.

Gupta, H. V., Kling, H., Yilmaz, K. K., and Martinez, G. F.: Decomposition of the mean squared error and NSE performance criteria: Implications for improving hydrological modelling, J. Hydrol., 377, 80–91, https://doi.org/10.1016/j.jhydrol.2009.08.003, 2009.

Hoffman, E. O. and Gardner, R. H.: Evaluation of Uncertainties in Environmental Radiological Assessment Models, in: Radiological Assessments: a Textbook on Environmental Dose Analysis, edited by: Till, J. E. and Meyer, H. R., U.S. Nuclear Regulatory Commission Washington, DC, Report No. NUREG/CR-3332, 1983.

Howard, J. L.: Artemisia tridentata subsp. Wyomingensis, in: Fire Effects Information System, U.S. Department of Agriculture, Forest Service, Rocky Mountain Research Station, Fire Sciences Laboratory (Producer), available at: https://www.fs.fed.us/database/feis/plants/shrub/arttriw/all.html (last access: 20 August 2018), 1999.

Keating, E. H., Doherty, J., Vrugt, J. A., and Kang, Q. J.: Optimization and uncertainty assessment of strongly nonlinear groundwater models with high parameter dimensionality, Water Resour. Res., 46, W10517, https://doi.org/10.1029/2009WR008584, 2010.

Kim, Y., Knox, R. G., Longo, M., Medvigy, D., Hutyra, L. R., Pyle, E. H., Wofsy, S. C., Bras, R. L., and Moorcroft, P. R.: Seasonal carbon dynamics and water fluxes in an Amazon rainforest, Glob. Change Biol., 18, 1322–1334, https://doi.org/10.1111/j.1365-2486.2011.02629.x, 2012.

Knick, S. T. and Dobkin, D. S.: Teetering on the Edge or Too Late? Conservation and Research Issues for Avifauna of Sagebrush Habitats, The Condor, 105, 611–634, https://doi.org/10.1650/7329, 2003.

Knox, R. G., Longo, M., Swann, A. L. S., Zhang, K., Levine, N. M., Moorcroft, P. R., and Bras, R. L.: Hydrometeorological effects of historical land-conversion in an ecosystem-atmosphere model of Northern South America, Hydrol. Earth Syst. Sci., 19, 241–273, https://doi.org/10.5194/hess-19-241-2015, 2015.

Krause, P., Boyle, D. P., and Bäse, F.: Comparison of different efficiency criteria for hydrological model assessment, Adv. Geosci., 5, 89–97, https://doi.org/10.5194/adgeo-5-89-2005, 2005.

Kwon, H., Pendall, E., Ewers, B. E., Cleary, M., and Naithani, K.: Spring drought regulates summer net ecosystem CO_2 exchange in a sagebrush-steppe ecosystem, Agr. Forest Meteorol., 148, 381–391, https://doi.org/10.1016/j.agrformet.2007.09.010, 2008.

Kwon, B., Kim, H. S., Jeon, J., and Yi, M. J.: Effects of Temporal and Interspecific Variation of Specific Leaf Area on Leaf Area Index Estimation of Temperate Broadleaved Forests in Korea, Forests, 7, 215, https://doi.org/10.3390/f7100215, 2016.

Lambrecht, S. C., Shattuckb, A. K., and Loik, M. E.: Combined drought and episodic freezing effects on seedlings of low- and high-elevation subspecies of sagebrush (*Artemisia tridentata*), Physiol. Plantarum, 130, 207–217, 2007.

LCC: Landscape Conservation Cooperatives: 2015 LCC Network Areas OGC Webservices, available at: https://www.sciencebase.gov/catalog/item/55c52e08e4b033ef5212bd75, last access: 21 April 2018.

LeBauer, D. S., Wang, D., Richter, K. T., Davidson, C. C., and Dietze, M. C.: Facilitating feedbacks between field measurements and ecosystem models, Ecol. Monogr., 83, 133–154, https://doi.org/10.1890/12-0137.1, 2013.

Leuning, R.: A critical appraisal of a combined stomatal-photosynthesis model for C_3 plants, Plant Cell Environ., 18, 339–355, 1995.

Li, C., Sun, O. J., Xiao, C., and Han, X.: Differences in Net Primary Productivity Among Contrasting Habitats in Artemisia ordosica Rangeland of Northern China, Range Ecol. Manage., 62, 345–350, https://doi.org/10.2111/07-084.1, 2009.

McArthur, E. D. and Plummer, A. P.: Biogeography and management of native western shrubs: a case study, Section Tridentatae of Artemisia, Great Basin Naturalist Memoirs, 2, 15, https://scholarsarchive.byu.edu/gbnm/vol2/iss1/15, 1978.

McIver, J. and Brunson, M.: Multidisciplinary, Multisite Evaluation of Alternative Sagebrush Steppe Restoration Treatments: The SageSTEP Project, Range Ecol. Manage., 67, 435–439, https://doi.org/10.2111/REM-D-14-00085.1, 2014.

Medvigy, D. M.: The state of the regional carbon cycle: Results from a coupled constrained ecosystem-atmosphere model, PhD Thesis, Harvard Univ., Cambridge, MA, 2006.

Medvigy, D. M. and Moorcroft, P. R.: Predicting ecosystem dynamics at regional scales: an evaluation of a terrestrial biosphere model for the forests of northeastern North America, Phil. Trans. R. Soc. B, 367, 222–235, https://doi.org/10.1098/rstb.2011.0253, 2012.

Medvigy, D., Wofsy, S. C., Munger, J. W., Hollinger, D. Y., and Moorcroft, P. R.: Mechanistic scaling of ecosystemfunction and dynamics in space and time: Ecosystem Demog-

raphy model version 2, J. Geophys. Res., 114, G01002, https://doi.org/10.1029/2008JG000812, 2009.

Medvigy, D., Jeong, S. J., Clark, K. L., Skowronski, N. S., and Schäfer, K. V. R.: Effects of seasonal variatio n of photosynthetic capacity onthe carbon fluxes of a temperate deciduous forest, J. Geophys. Res.-Biogeo., 118, 1703–1714, https://doi.org/10.1002/2013JG002421, 2013.

Miller, P. A. and Smith, B.: Modelling Tundra vegetation response to recent Arctic warming, Ambio, 41, 281–291, 2012.

Miller R. F., Knick, S. T., Pyke, D. A., Meinke, C. W., Hanser, S. E., Wisdom, M. J., and Hild, A. L.: Characteristics of sagebrush habitats and limitations to long-term conservation, in: Greater sage-grouse–ecology and conservation of a landscape species and its habitats, edited by: Knick S. T. and Connelly, J. W., Studies in avian biology no. 38, University of California Press, Berkeley, CA, USA, 145–185, 2011.

Mitchell, J. J., Glenn, N. F., Sankey, T. T., Derryberry D. R., Anderson, M. O., and Hrusk, R. C.: Small-footprint Lidar Estimations of Sagebrush Canopy Characteristics, Photogramm. Eng. Rem. S., 77, 521–530, 2011.

Mo, X., Chen, J. M., Ju, W., and Black, T. A.: Optimization of ecosystem model parameters through assimilating eddy covariance flux data with an ensemble Kalman filter, Ecol. Model., 217, 157–173, https://doi.org/10.1016/j.ecolmodel.2008.06.021, 2008.

Moorcroft, P. R.: Recent advances in ecosystem-atmosphere interactions: an ecological perspective, Phil. Trans. R. Soc. B, 270, 1215–1227, https://doi.org/10.1098/rspb.2002.2251, 2003.

Moorcroft, P. R., Hurtt, G. C., and Pacala, S. W.: A method for scaling vegetation dynamics: the Ecosystem Demography model (ED), Ecol. Monogr., 71, 557–586, https://doi.org/10.1890/0012-9615(2001)071[0557:AMFSVD]2.0.CO;2, 2001.

Nash, J. E. and Sutcliffe, J. V.: River flow forecasting through conceptual models, Part I – A discussion of principles, J. Hydrol., 10, 282–290, 1970.

Oleson, K., Lawrence, D. M., Bonan, G. B., Drewniak, B., Huang, M., Koven, C. D., Levis, S., Li, F., Riley, W. J., Subin, Z. M., Swenson, S. C., Thornton, P. E., Bozbiyik, A., Fisher, R., Heald, C. L., Kluzek, E., Lamarque, J.-F., Lawrence, P. J., Leung, L. R., Lipscomb, W., Muszala, S., Ricciuto, D. M., Sacks, W., Sun, Y., Tang, J., and Yang, Z.-L.: Technical Description of version 4.5 of the Community Land Model (CLM), NCAR Technical Note NCAR/TN-503+STR, Boulder, Colorado, 420 pp., 2013.

Olsoy, P. J., Mitchell, J. J., Levia, D. F., Clark, P. E., and Glenn, N. F.: Estimation of big sagebrush leaf area index with terrestrial laser scanning, Ecol. Indic., 61, 815–821, https://doi.org/10.1016/j.ecolind.2015.10.034, 2016.

Pacala, S. W., Canham, C. D., and Silander Jr., J. A.: Forest models defined by field measurements. I. The design of a northeastern forest simulator, Can. J. For. Res., 23, 1980–1988, 1993.

Pandit, K: Modified source codes for ED2 with shrub parameters, Zenodo, https://doi.org/10.5281/zenodo.3461233, 2019.

Pereira, F. F., Farinosi, F., Arias, M. E., Lee, E., Briscoe, J., and Moorcroft, P. R.: Technical note: A hydrological routing scheme for the Ecosystem Demography model (ED2+R) tested in the Tapajós River basin in the Brazilian Amazon, Hydrol. Earth Syst. Sci., 21, 4629–4648, https://doi.org/10.5194/hess-21-4629-2017, 2017.

Qi, Y., Dennison, P. E., Jolly, W. M, Kropp, R. C., and Brewer, S. C.: Spectroscopic analysis of seasonal changes in live fuel moisture content and leaf dry mass, Remote Sens. Environ., 150, 198–206, https://doi.org/10.1016/j.rse.2014.05.004, 2014.

Qi, Y., Ustin, S. L., and Glenn, N. F.: Imaging Spectroscopic Analysis of Biochemical Traits for Shrub Species in Great Basin, USA, Remote Sens., 10, 1621, https://doi.org/10.3390/rs10101621, 2018.

Quan, X., He, B., and Li, X.: A Bayesian Network-Based Method to Alleviate the Ill-Posed Inverse Problem: A Case Study on Leaf Area Index and Canopy Water Content Retrieval, IEEE T. Geosci. Remote, 33, 6507–6517, https://doi.org/10.1109/TGRS.2015.2442999, 2015

Reichstein, M., Falge, E., Baldocchi, D., Papale, D., Aubinet M., Berbigier P., Bernhofer, C., Buchmann, N., Gilmanov, T., Granier, A., Grünwald, T., Havránková, K., Ilvesniemi, H., Janous, D., Knohl, A., Laurila, T., Lohila, A., Loustau, D., Matteucci, G., Meyers, T., Miglietta, F., Ourcival, J. M., Pumpanen, J., Rambal, S., Rotenberg, E., Sanz, M., Tenhunen, J., Seufert, G., Vaccari, F., Vesala, T., Yakir, D., and Valentini, R.: On the separation of net ecosystem exchange into assimilation and ecosystem respiration: review and improved algorithm, Glob. Change Biol., 11, 1424–39, https://doi.org/10.1111/j.1365-2486.2005.001002.x, 2005.

Richardson, A. D., Williams, M., Hollinger, D. Y., Moore, D. J. P., Dail, D. B., Davidson, E. A., Scott, N. A., Evans, R. E., Hughes, H., Lee, J. T., Rodrigues, C., and Savage, K.: Estimating parameters of a forest ecosystem C model with measurements of stocks and fluxes as joint constraints, Oecologia, 164, 25–40, https://doi.org/10.1007/s00442-010-1628-y, 2010.

Schlaepfer, D. R., Lauenrotha, W. K., and Bradford, J. B.: Modeling regeneration responses of big sagebrush (Artemisia tridentata) to abiotic conditions, Ecol. Model., 286, 66–77, https://doi.org/10.1016/j.ecolmodel.2014.04.021, 2014.

Schmidtlein, S., Tichy, L., Feilhauer, H., and Faude, U.: A brute-force approach to vegetation classification, J. Veg. Sci., 21, 1162–1171, https://doi.org/10.1111/j.1654-1103.2010.01221.x, 2010.

Schroeder, M. A., Aldridge, C. L., Apa, A. D., Bohne, J. R., Braun, C. E., Bunnell, S. D., Connelly, J. W., Deibert, P. A., Gardner, S. C., Hilliard, M. A., Kobriger, G. D., McAdam, S. M., McCarthy, C. W., McCarthy, J. J., Mitchell, D. L., Rickerson, E. V., and Stiver, S. J.: Distribution of Sage-Grouse in North America, The Condor, 106, 363–376, https://doi.org/10.1650/7425, 2004.

Schwantes, A. M., Swenson, J. J., and Jackson, R. B.: Quantifying drought-induced tree mortality in the open canopy woodlands of central Texas, Remote Sens.Environ., 181, 54–64, https://doi.org/10.1016/j.rse.2016.03.027, 2016.

Sellers, P. J., Berry, J. A., Collatz, G. J., Field, C. B., and Hall, F. G.: Canopy reflectance, photosynthesis, and transpiration, III. A reanalysis using improved leaf models and a new canopy integration scheme, Remote Sens. Environ., 42, 187–216, https://doi.org/10.1016/0034-4257(92)90102-P, 1992.

Seyfried, M. S., Harris, R., Marks, D., and Jacob, B.: A geographic database for watershed research: Reynolds Creek Experimental Watershed, Idaho, USA, Tech. Bull. NWRC 2000-3, 26 pp., Northwest Watershed Res. Cent., Agric. Res. Serv., U.S. Dep. of Agric., Boise, Idaho, 2000

Sitch, S., Smith, B., Prentice, I. C., Arneth, A., Bondeau, A., Cramer, W., Kaplans, J. O., Levis, S., Lucht, W., Sykes, M. T., Thonicke, K., and Venevsky, S.: Evaluation of ecosystem dynamics, plant geography and terrestrial carbon cycling in the LPJ dynamic vegetation model, Glob. Change Biol., 9, 161–185, 2003.

Skamarock, W. C., Klemp, J. B., Dudhia, J., Gill, D. O., Barker, D. M., Duda, M. G., Huang, X., Wang, W., and Powers, J. G.: A Description of the Advanced Research WRF Version 3. NCAR Technical Note NCAR/TN-475+STR, https://doi.org/10.5065/D68S4MVH, 2008.

Smith, B., Trentice, C. I., and Sykes, M. T.: Representation of vegetation dynamics in the modelling of terrestrial ecosystems: comparing two contrasting approaches within European climate space, Global Ecol. Biogeogr., 10, 621–637, 2001.

Steinberg, P. D.: Artemisia arbuscula, iFire Effects Information System, U.S. Department of Agriculture, Forest Service, Rocky Mountain Research Station, Fire Sciences Laboratory (Producer), available at: https://www.fs.fed.us/database/feis/plants/shrub/artarb/all.html (last access: 27 July 2019), 2002.

Stephenson, G. R. (Ed.): CZO Dataset: Reynolds Creek – Geology, Soil Survey, Vegetation, GIS/Map Data (1960–1970), available at: http://criticalzone.org/reynolds/data/dataset/3722/, last access: 18 May 2018.

Sturges, D. L.: Soil water withdrawl and root characteristics of Big Sagebrush, Am. Midl. Nat., 98, 257–274, 1977.

Tabler, R. D.: The root system of Artemisia tridentata at 9,500 feet in Wyoming, Ecology, 45, 633–636, 1964.

Trugman, A. T., Fenton, N. J., Bergeron, Y., Xu, X., Welp, L. R., and Medvigy, D.: Climate, soil organic layer, and nitrogen jointly drive forest development after fire in the North American boreal zone, J. Adv. Model. Earth Syst., 8, 1180–1209, https://doi.org/10.1002/2015MS000576, 2016.

USDA: Plant materials Technical Note No. MT-114, Natural Resources Conservation Service, United States Department of Agriculture, August 2016, 2016.

USDA: Soil Survey Staff, Natural Resources Conservation Service, United States Department of Agriculture, Web Soil Survey, available at: https://websoilsurvey.sc.egov.usda.gov/, last access: 28 March, 2018a.

USDA: The PLANTS Database, National Plant Data Team, Greensboro, NC 27401-4901 USA, available at: http://plants.usda.gov, last access: 20 August, 2018b.

Wambura, F. J., Ndombab, P. M., Kongob, V., and Tumboc, S. D.: Uncertainty of runoff projections under changing climate in Wami River sub-basin, J. Hydrol.-Reg. Studies, 4, 333–348, 2015.

Wang, D., LeBauer, D., and Dietze, M.: Predicting yields of short-rotation hybrid poplar (Populus spp.) for the United States through model–data synthesis, Ecol. Appl., 23, 944–958, 2013.

Waring, B. G., Averill, C., and Hawkes, C. V.: Differences in fungal and bacterial physiology alter soil carbon and nitrogen cycling: insights from meta-analysis and theoretical models, Ecol. Lett., 16, 887–894, https://doi.org/10.1111/ele.12125, 2016

Weiss, A. and Norman, J. M.: Partitioning solar radiation into direct and diffuse, visible and near-infrared components, Agr. Forest Meteorol., 34, 205–213, 1985.

Wolf, A., Callaghan, T. V., and Larson, K.: Future changes in vegetation and ecosystem function of the Barents Region, Clim. Change, 87, 51–73, 2008.

Zaehle, S., Sitch, S., Smith, B., and Hatterman, F.: Effects of parameter uncertainties on the modeling of terrestrial-biosphere dynamics, Global Biogeochem. Cy., 19, GB3020, https://doi.org/10.1029/2004GB002395, 2005.

Zhang, K., de Almeida Castanho, A. D., Galbraith, D. R., Moghim, S., Levine, N. M., Bras, R. L., Coe, M. T., Costa, M. H., Malhi, Y., Longo, M., Knox, R. G., McKnight, S., Wang, J., and Moorcroft, P. R.: The fate of Amazonian ecosystems over the coming century arising from changes in climate, atmospheric CO_2, and land use, Glob. Change Biol., 21, 2569–2587, https://doi.org/10.1111/gcb.12903, 2015.

Zhang, K., Ma. J., Zhu, G., Ma, T., Han, T., and Feng, L. L.: Parameter sensitivity analysis and optimization for a satellite-based evapotranspiration model across multiple sites using Moderate Resolution Imaging Spectroradiometer and flux data, J. Geophys. Res.-Atmos., 122, 230–245, https://doi.org/10.1002/2016JD025768, 2017.

Zhang, Y, Guanter, L., Berry, J. A., Joiner, J., Tol, C. V. D., Huete, A., Gitelson, A., Voigt, M., and Kohler, P.: Estimation of vegetation photosynthetic capacity from space-based measurements of chlorophyll fluorescence for terrestrial biosphere models, Glob. Change Biol., 20, 3727–3742, https://doi.org/10.1111/gcb.12664, 2014.